Biosynthesized rGO@ZnO Nanocomposite for Bovine Serum Albumin Detection

A DISSERTATION

SUBMITTED IN THE PARTIAL FULFILLMENT OF THE REQUIREMENT

FOR THE AWARD OF THE DEGREE OF MASTER OF TECHNOLOGY

in

POLYMER TECHNOLOGY

Submitted by

PALAK GARG 2K18/PTE/04

Under the supervision of

Prof. D KUMAR

DEPARTMENT OF APPLIED CHEMISTRY
DELHI TECHNOLOGICAL UNIVERSITY
(Govt. of NCT of Delhi)
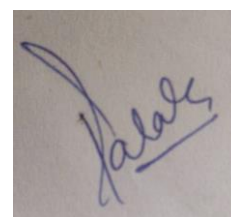Shahbad Daulatpur, Main Bawana Road,
Delhi-110042

DELHI TECHNOLOGICAL UNIVERSITY
(Formerly Delhi College of Engineering)
Bawana Road, Delhi-110042

<u>CANDIDATE'S DECLARATION</u>

I, Palak Garg, 2K18/PTE/04 student of M.Tech hereby declare that the project Dissertation titled "Biosynthesized rGO@ZnO Nanocomposite for Bovine Serum Albumin Detection" which is submitted by me to the Department of Applied Chemistry, Delhi Technological University, Delhi in the partial fulfillment of the requirement for the award of the degree of Master of Technology (Polymer Technology) is original and not copied from any source without proper citation. This work has not previously formed the basis for the award of any Degree, Diploma Associateship, Fellowship or other similar title or recognition.

Place:Delhi   **Palak Garg**

Date: 21/08/2020   **2K18/PTE/04**
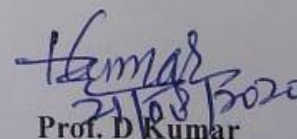
Department of Applied Chemistry
DELHI TECHNOLOGICAL UNIVERSITY
(Formerly Delhi College of Engineering)
Bawana Road, Delhi-110042

CERTIFICATE

I/We hereby certify that the project Dissertation titled "Biosynthesized rGO@ZnO Nanocomposite for Bovine Serum Albumin Detection" which is submitted by **Palak Garg, 2K18/PTE/04,** Department of Applied Chemistry, Delhi Technological University, Delhi in partial fulfillment of the requirement for the award of the Master of Technology (Polymer Technology) is a record of the project work carried out by the student under my/our supervision. To the best of my/our knowledge, this work has not been submitted in part or full for any Degree or Diploma to this University or elsewhere.

Place: Delhi

Date: 21/08/2020

Prof. D Kumar

(SUPERVISOR)

ACKNOWLEDGEMENT

ABSTRACT

Bovine serum albumin (BSA) is a globular protein that plays a pivotal role in the delivery of fatty acid/amino acid. The presence of multiple binding sites in BSA allows it to interact with many inorganic, organic molecules, ionic metals, and radicals. The reduction of BSA may cause various diseases in cattle families, thus making the quantification of BSA crucial.

In the present work, efforts have been made to fabricate an immunosensor for the detection of BSA using reduced graphene oxide@zinc oxide nanocomposite (rGO@ZnO). The nanocomposite has been synthesized *via* a biosynthetic approach, where *Aloe vera* leaf extract was used as a reducing agent. The characterization of the nanocomposite was conducted using UV-visible spectroscopy, FT-IR, Zeta Potential and TGA techniques. Further, the rGO@ZnO nanocomposite was deposited electrophoretically on indium tin oxide coated glass substrate, followed by the immobilization of antibodies. The fabricated rGO@ZnO biosensor exhibits a good linear range (0.001 to 30 ng mL^{-1}), low detection limit with acceptable selectivity and stability.

Keywords: Graphene Oxide, ZnO, *Aloe vera,* BSA, Nanocomposite.

List of Contents

List of tables

List of figure captions

<u>List of abbreviations</u>

BSA	Bovine Serum Albumin
CE	Counter Electrode
CV	Cyclic Voltammetry
DNA	Deoxyribonucleic Acid
DPV	Differential Pulse Voltammetry
EDC	1-ethyl-3-(3-dimethyl amino) propyl carbodiimide
FT-IR	Fourier transform infrared spectroscopy
GO	Graphene Oxide
HSA	Human Serum Albumin
ITO	Indium Tin Oxide
NHS	N-hydroxy succinimide
NMO	Nanostructured Metal Oxide
PBS	Phosphate Buffered Saline
RE	Reference Electrode
rGO	Reduced graphene oxide
TGA	Thermogravimetric analysis
UV-Vis	Ultra-Violet Visible Spectroscopy
WE	Working Electrode
ZnO	Zinc Oxide

1. INTRODUCTION

Bovine Serum Albumin (BSA) is a cow protein that plays a vital role in the circulation of many endogenous and exogenous compounds into vertebrate blood to maintain the osmotic pressure of plasma [1]. BSA is composed of 17 cross-linked cysteine residue, 1 free cysteine and 582 amino acid residue [2]. The traditional methods used for BSA detection are resonance light scattering[3], [4], voltammetry assays[5], surface-enhanced plasma resonance[6], surface-enhanced Raman spectroscopy[7], near-infrared reflection spectroscopy[8], fluorimetric determination[9], circular dichroic[10], spectrophotometry methods etc. These methods take long duration times, use large volumes of reagents and sometimes also show lack of sensitivity. Therefore, there is an urgent need to develop a simple, sensitive, cost-effective and easy to use the device for the recognition of BSA. In this context, biosensors can play a pivotal role in the detection of target analytes with greater sensitivity and selectivity[11]. In biosensors, the generation of information is done by the measurement of electrical properties from biological systems, i.e., bio-electrochemical, which serves as a transduction element. These devices act as recognizing elements due to their specific binding and bio-catalytic activities. An immunosensor utilizes antibodies or antigens to generate bio-electrochemical responses. Antibodies are immobilized on the surface in order to detect the antigens. Biosensors allow the detection of biomolecules with high affectability, selectivity, with a low response time[12].

For the fabrication of biosensor, the selection of effective transducer surfaces that bind the recognition molecule and providing faster access to the analyte is essential. Nowadays, graphene has attracted much interest in the development of biosensors. Graphene is a 2-D sheet of sp^2 reinforced carbon and is a reasonable material for robust electrode because of its striking features like large interfacial surface area, electrical conductivity, quick electron move, simplicity of functionalization, and large scale manufacturing. Graphene provides a suitable microenvironment for protein and provide an immediate electron move of the biomolecules at the terminal surface. Metal nanoparticles utilized as successful immobilization platforms for the improvement of the electrochemical properties of the biosensors [13]. Incorporation of graphene with

different metal nanop[articles enhances the electrochemical catalytic activity compared to bare graphene. The graphene-metal nanocomposite gives a more significant electrochemical dynamic surface, which brings about the assimilation of more biomolecules and expands the electron transfer between the electrode surface and the redox mediator [14]. Graphene oxide-metal oxide nanocomposite has shown excellent capabilities to stimulate direct electron transfer of the entrapped bio-molecules and keeping the bioactivity for a long time [15]. Nanostructured metal oxides (NMO), due to their unique physical, chemical and catalytic properties have aroused the interest as immobilization platforms in biosensors. Notable NMO of titanium, iron, tin, cerium, zirconium, zinc and magnesium have found fascinating functional biocompatibility, nano-morphological, and electrochemical properties. NMO shows improved electron efficiency and high adsorption abilities and provides suitable microenvironments for the immobilization of biomolecules[16]. Nanostructured ZnO has a vast explicit surface territory, quick electron moveability, solid retention to proteins, great chemical stability and ideal biocompatibility [17].

Further, the chemical reduction of GO to rGO tends to form irreversible aggregation due to strong vander Waals forces of attraction between graphene planes that create a bottleneck and confines its ability. Moreover, the chemical reduction is highly toxic due to the chemical reducing agents used like hydrazine, dimethylhydrazine, hydroquinone, etc. [18]–[20]. Recently, the reduction of graphene oxide using plant extract has attracted a great deal of attention among the researchers. This method is eco-friendly, cost-effective and sustainable than any other chemical reducing agents. Phytochemicals present in plant extracts contain biomolecules including amino acids, vitamins, pectin, alcoholic compounds, proteins, enzymes act as reducing agents [21].

In this work, we have prepared an electrochemical immunosensor for BSA detection using rGO@ZnO nanocomposite, which was biosynthesized using plant extract, i.e, *aloe vera* leaves extract acting as a reducing agent. The biosynthesized nanocomposite was electrophoretically deposited onto ITO covered glass substrate. The electrochemical results show that fabricated biosensors have good sensitivity with a low limit of detection.

2. LITERATURE REVIEW

2.1 Biosensor

IUPAC defines biosensors as "integrated receptor-transducer devices, which are able to provide selective quantitative or semi-quantitative analytical information using a biological recognition element.[22]"
Biosensors are mainly comprised of two elements:

1. Bioreceptors: Biological element which is sensitive to recognizing the analyte.

2. Transducers: Converts a biochemical signal into an electrical signal.
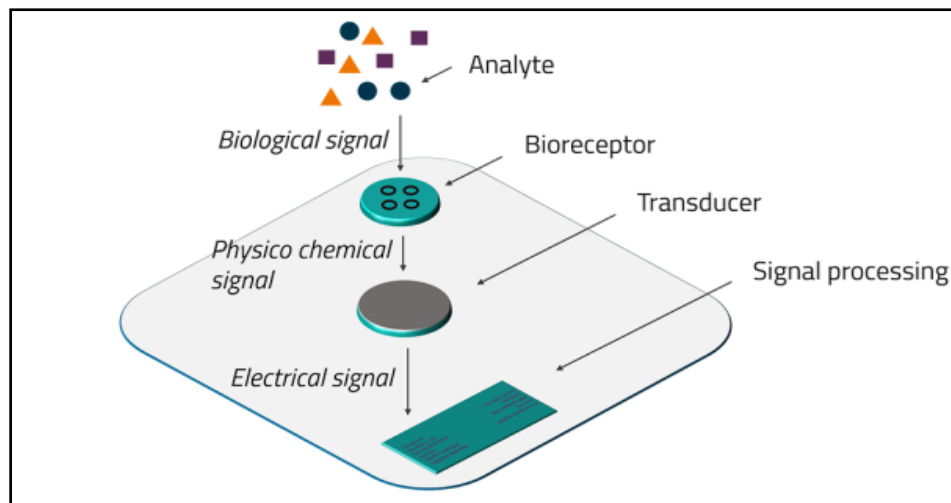
Fig.1.1 Schematic representation of a biosensor.

The bio-receptors that are generally used in biosensors are DNA, enzymes, proteins, antigen, etc. Based on transducing elements, biosensors are classified into four types: Electrochemical, Piezoelectric, Optical and Thermal biosensor. Among these biosensors, electrochemical biosensor has gained special attention due to its ability to replace bulky and expensive apparatus. Also, they show excellent selectivity, sensibility, stability, reproducibility, low response time and quick maintenance at very low cost[16].

2.1.1 Electrochemical Biosensors

According to IUPAC (1999), "an electrochemical biosensor is a self-contained integrated device that is capable of providing specific quantitative or semi-quantitative analytical information using a biological recognition element which is kept in direct spatial contact with an electrochemical transduction element". Electrochemical sensing usually contains a working electrode (WE), a reference electrode (RE), and a counter electrode (CE). The reactions are detected only on the electrode surface [23].

WE is the transduction element in the EC system; here the biochemical reaction takes place. The CE performs as a connection to the electrolytic solution for applying current to the WE. RE helps to maintain a desirable and stable potential. A redox reaction of the molecule takes place at the electrode surface, where electrons relocation happens from the analyte to the WE or from the WE to the analyte. If WE is driven to a positive potential, then an oxidation reaction occurs and a reduction reaction occurs, if the WE is driven to a negative potential [24].

EC biosensors can be classified into four categories:

1. Amperometric biosensors: estimate the current change generated from the electrochemical oxidation and decrease of an electroactive species. It is performed when a steady potential is applied at CE.
2. Potentiometric biosensors: measure the electrical potential of an electrode to provide an analytical signal.
3. Conductometric biosensors: measure the electrical conductivity between couples of metal cathodes because of a biological element.
4. Electrochemical impedance spectroscopy: In this case, the current of the cell is measured by an AC potential to an EC cell [16].

2.1.2 Electrochemical Method

The electrochemical (EC) method is used for the determination of analytes from the matrix. EC techniques are of two types, i.e., non-interfacial and interfacial methods. Conductometry is a non-interfacial method where measurement of the solution is taken as a whole. When AC is applied, there is no electrode polarization. Whereas the interfacial method responds to the presence of analyte on the electrode surface, which results in the disturbance of an electric signal that can be quantified. Interfacial methods are again divided into two groups: Static and Dynamic methods. In the static method, an electric current is zero, and there is no disturbance, while the dynamic method involves a redox reaction where electron transfer occurs between the analyte and WE. The dynamic method utilizes current flow, which can be used for the development of biosensors and nanostructured materials [25].

2.1.3 Cyclic Voltammetry

In CV, the potential is measured to and fro between the two likely cutoff points while the current circles all through the cycle are recorded. Fig. 1.2, shows the CV graph plotted between current *vs* potential. CV is utilized to decide the redox procedures of different analytes. The redox reaction takes place between WE and the electrolyte solution. Thus, current is recorded at WE during potential scan against constant RE. Randles- Sevcik equation can be used to quantify the peak current in the CV.

$$I_p = (2.99*10^5) \, \alpha^{1/2} \, n^{3/2} \, A \, C \, D^{1/2} \, \upsilon^{1/2}$$

where I_p is peak current; A is electrode area; α is electron transfer coefficient; n is no. of electrons, C concentration; D is the diffusion coefficient; υ is scan rate. Hence, CV helps to analyze the no. of electrons reduced/oxidized, diffusion coefficient, concentration and redox potential for analyte [16].
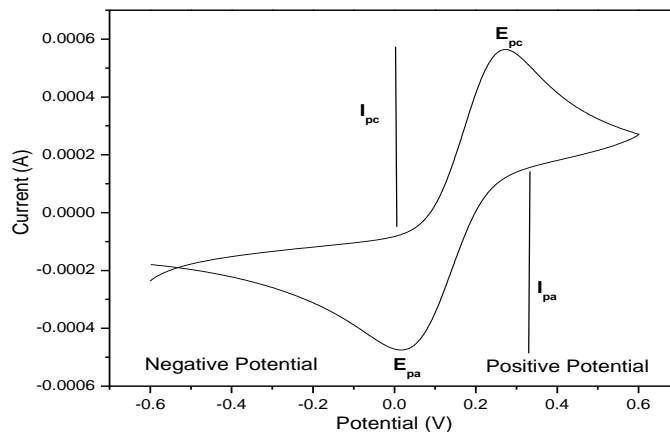
Fig. 1.2 Cyclic voltammogram of rGO@ZnO/ITO at scan rate 50 mV/s.

2.1.4 Differential Pulse Voltammetry

DPV is defined as "an electrochemical technique where the cell current is measured as a function of time and as a function of the potential between the WE and RE electrodes". The potential is varied using pulses of increasing amplitude and the current is sampled before and after each voltage pulse. It is a voltammetry technique that provides enhanced selectivity for observing the redox process as compared to CV. It is an irreversible system and shows slow reaction kinetics [25].

2.2 Bovine Serum Albumin

Albumin is a vital protein that helps in maintaining nutritional balance and plasma pressure. Since proteins are functioning as a transporter in a body, therefore recognition of these macro-molecules is necessary[26]. BSA is a globular cow protein having a molecular weight of 68.8 kDa approx and the heart-formed structure has 3 homologous spaces I-III and every area comprises of 2 sub-areas, A and B with one of a kind restricting properties. In the sub-space IB and sub-areas IIA, BSA contains 2 tryptophan amino acid deposits as 134 and 212 individually. Circulatory, healthful and physiological elements of BSA make them fundamental bio-macromolecules going about as a transporter for carrying and conveying distinctive exogenous and endogenous

substances, particles, unsaturated fats, little atoms, for example, pharmaceuticals in the body. BSA has been utilized as a supplement in cell and microbial culture while in molecular biology, it is utilized to settle some limitation enzymes during the assimilation of DNA and to forestall attachment of the protein to response tubes, pipette tips and different vessels.

Human Serum Albumin (HSA) is the protein present in the human circulatory framework richly. Human wellbeing is firmly identified with the HSA focus in blood plasma or other natural liquids. HSA and BSA have high structural similarity. BSA is explored as a modal protein in various fields[27].
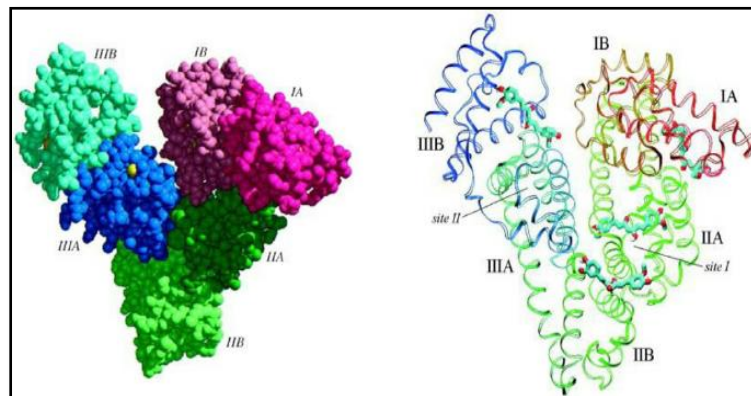
Fig.2.2Structure of BSA and HSA[26].

2.3 Graphene

Graphene has a honeycomb structure, having a 2D sheet of a carbon atom and known to be the thinnest material till date. The remarkable electronic, mechanical, optical, thermal, excellent conductivity, easy functionalization properties and mass production make graphene a favorable material for biosensors. Many thermal, mechanical and other methods have been proposed to synthesize graphene but the most economical way for mass production is by chemical reduction of graphite to GO.

GO is generally synthesized via Hummer's method, where certain oxidants are used like concentrated sulphuric acid, potassium permanganate and nitric acid for the oxidation of graphite [28]. GO has a non-planar structure with a distorted sp^2 carbon network as it is loaded with oxygenated groups having epoxy and hydroxyl groups. Additionally,

carbonyl and carboxyl gatherings put at sheet edges on sp^2 hybridized carbon. rGO is functionalized graphene sheets, which are commonly synthesized by chemical reduction of GO. A high density of defects is created in GO in order to turn into rGO, which leads to higher electrochemical activity and helpful in developing electrochemical biosensors[16]. The rGO exhibits excellent properties like solvent dispersibility, optical, mechanical, thermal stability compared to GO and graphene.

Chemical as well as bio-reduction of GO sheets, are being done using several reducing agents. Chemical reducing agents include sodium borohydride, hydrazine etc, whereas for bio-reduction plants, extracts are being used. The rGO becomes less hydrophilic compared to GO due to the removal of oxygen atoms. Plants have properties to reduce metallic ions biologically. Due to this property, plants are considered to be an environment-friendly route for synthesizing the nanoparticles. Plants contain numerous bioactive terpenoids, phenolic acids, sugars, proteins and polyphenols that help in reducing metal-ions and stabilizing them [19].

Generally, graphenes are reduced by chemical methods such as by hydrazines or by its derivatives. Therefore, profoundly harmful and temperamental hydrazine or its subordinates are to be taken care of with incredible safeguards. Accordingly, there is a developing requirement for the improvement of condition well-disposed blend that doesn't utilize toxic synthetic substances. The bio-reduction of GO has been suggested as an eco-friendly route and alternative to chemical and physical methods. GO can be reduced using microbes as well as plants. Since high specifications are used in microbes to maintain their pH, temperature, humidity, culture preparation and culture maintenance etc, which takes the complex and a longer period to process. Therefore, plants are used as a simpler technique, cheaper and time-saving method for bio-reduction[29].

Aloe vera plant has been used as a medicinal purpose across the globe. It is one of the most cultivated and household plants. It contains various phytochemicals such as polymannas, anthraquinone, anthros, C-glycosides, emodin, lectins etc. which demonstrates their excellent capability as reducing agents in metal salts [21]. It is readily available, low cost and substitute for hazardous chemicals. It acts as a green, reducing agent that helps in enhancing current density and decrease in charge transfer resistance. It also enhances the surface area.
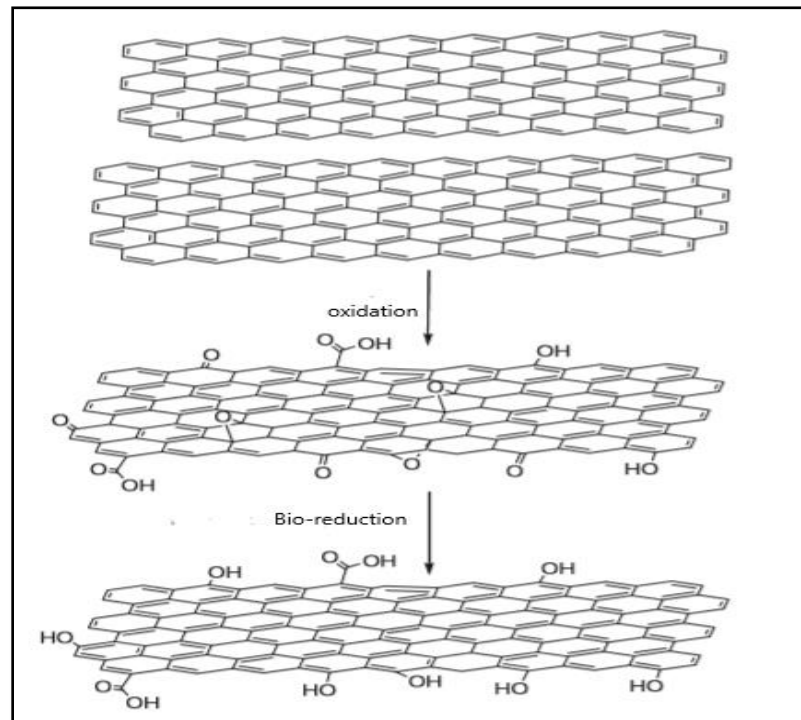
Fig. 2.3. Formation of GO by oxidation of graphite and rGO by bio-reduction of GO.

2.4 Zinc Oxide

ZnO has many attractive properties with a wide range of applications. Semiconductor ZnO has bandgap 3.37 eV. Nanostructured ZnO owns a large surface area, chemical stability, non- toxic, and shows good biocompatibility. ZnO's isoelectric point is about 9.5 and shows a high electron transfer. Thus, nano structured ZnO is worthy for protein absorption with a low isoelectric point as protein immobilization is taken by electrostatic interaction. Nanostructured ZnO also offers lower fabrication costs as compared to other nanostructured materials [17].

2.5 rGO@ZnO Nanocomposite

rGO shows distinct properties such as high surface area, good optical transparency, electron confinement effects, electrochemical modulation, high thermal as well as chemical stability and high mechanical flexibility. ZnO has environment-friendly nature, biological compatibility, high chemical stability and economical to pockets. Thus, when ZnO is incorporated into rGO, the nanocomposite properties result in enhanced conductivity, electron stability, cost-effective, non- toxic in nature, biocompatible as well as the increased sensitivity of the electrochemical biosensor [30]

3. MATERIALS AND METHODS

3.1 Materials Required

Graphite powder, zinc nitrate ($Zn(NO_3)_2$); sodium chloride (NaCl); hydrogen peroxide (H_2O_2); sulphuric acid (H_2SO_4); hydrogen chloride (HCl), potassium permanganate ($KMnO_4$); bovine serum albumin(BSA), anti-BSA were purchased from Sigma Aldrich.

3.2 Preparation of *Aloe Vera* Extract

The *Aloe Vera* leaves were collected from the DTU campus, Delhi, India. The fresh plant leaves were washed altogether under running water and afterward slit into little segments. 25g of *aloe vera* leaves pieces were heated at 50-60°C in100 mL of distilled water with continuous stirring for 2h. The prepared extract was filtered using Whatman filter paper.
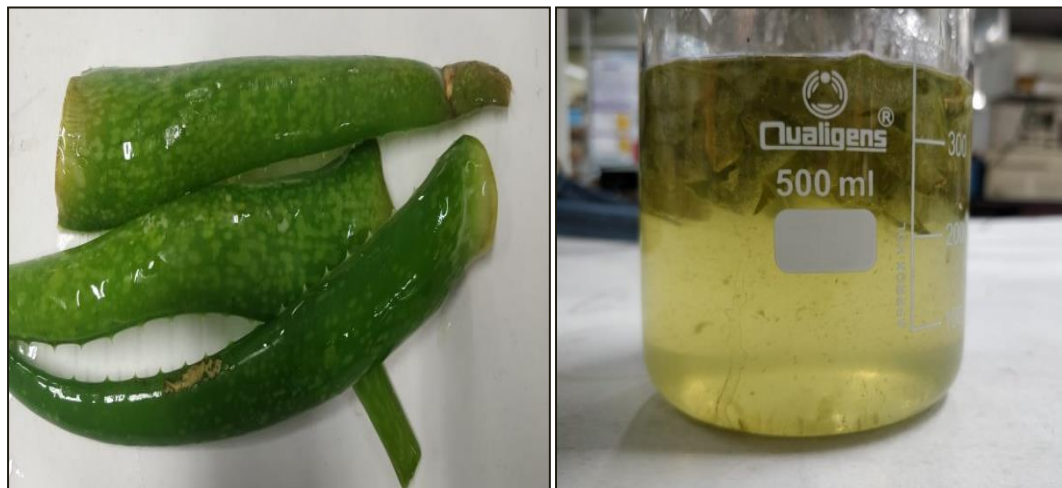
Fig 3.1 Images showing (a) *Aloe Vera* leaves (b) *Aloe vera* leaves extract.

3.3 Synthesis of Graphene Oxide (GO)

GO was synthesized by modified Hummer's method with slight modification. Graphite powder was grounded with NaCl in a mortar and dissolved in distilled H_2O. The grounded graphite powder was filtered and dried for 6 h at $90°C$. The powder was broken down in sulfuric acid under magnetic stirrer for 8 h and potassium permanganate was gradually included while the solution was kept at $20°C$. The solution's temperature was rose to $40°C$ for 30 min and afterward to $70°C$ for 45 min. At long last, the reaction was ended by gradually adding 200 mL distilled water and 10 mL hydrogen peroxide. The final solution was washed a few times with distilled water and hydrogen chloride. The product left was dried at $60°C$ for 24 h and got as black powder is graphene oxide.

3.4 Biosynthesis of rGO@ZnO nanocomposite

Initially, 5mL of *Aloe Vera e*xtract has been added to 0.5g zinc nitrate at $50-60°C$. Then, prepared GO suspension was added to the original solution with continuous stirring. The solution was heated until the paste was obtained. The paste was carefully transferred to the crucible and heated until powder material was obtained.

Fig 3.2. Image showing rGO@ZnO nanocomposite

3.5 Electrode Preparation

Electrophoretic deposition (EPD) was used for electrode preparation. The solution of 2 mg rGO@ZnO nanocomposite in 25 mL of distilled water and 5mL of ethanol was prepared and further sonicated for 1 h. Then, this solution was added to Milli-Q water in a 1:10 ratio and again sonicated for 15 min. After that, EPD was done on an ITO coated glass substrate at 10V for 10 sec.
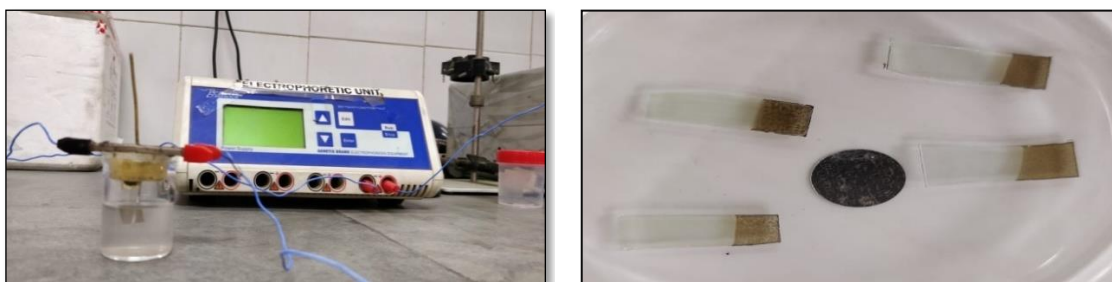
Fig. 3.3. Images showing (a) pictorial representation of EPD (b) deposition of rGO@ZnO nanocomposite onto ITO electrode.

3.6 Bioelectrode Fabrication

The prepared rGO@ZnO/ITO electrodes were immobilized with the anti-BSA using EDC-NHS as the crosslinker. The rGO@ZnO/ITO electrodes were modified with EDC (10 µL, 5 mM) and NHS (10 µL, 5mM) and placed in a humidity chamber at room temperature. After an hour, electrodes were washed with a PBS buffer of 7.2 pH. Further, the electrodes were immobilized with 10 µg/mL anti-BSA and kept for 6 h in a humid chamber at 4°C.
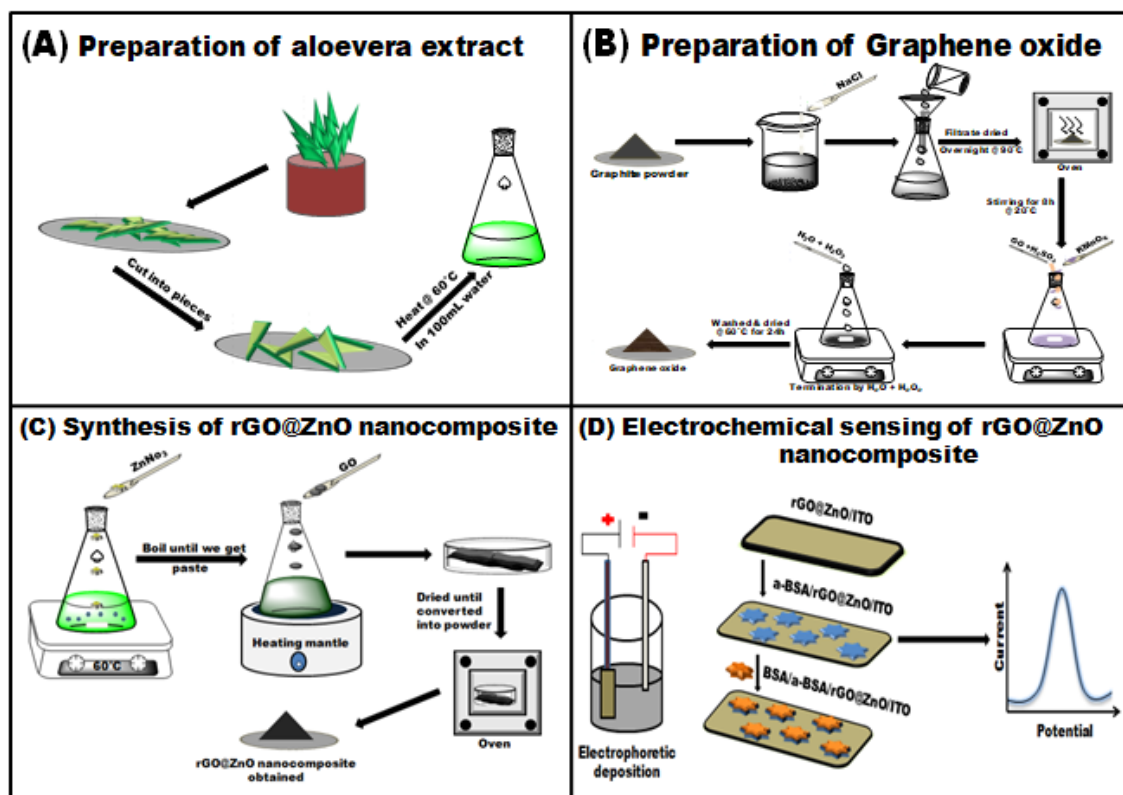
Fig. 3.4 Schematic showing (A) preparation of *Aloe Vera* extract (B) Preparation of GO (C) Synthesis of the rGO@ZnO nanocomposite. (D) Electrochemical sensing of the rGO@ZnO nanocomposite.

3.7 Instrumentation Techniques

FT-IR spectroscopy has been carried out using the Nicolet^{TM} iS10 FTIR spectrometer at 25°C in the frequency region of 400-4000 cm^{-1}. Thermal studies were carried out to analyze the thermal degradation of samples in the range 25 to 900°C at the pace of 10°C/min in nitrogen conditions using thermogravimetric analysis (TGA 4000, PerkinElmer). UV-Vis absorption study was done by a UV-Vis spectrophotometer (Perkin-Elmer model UV-260). Electrochemical studies of the electrode were carried out by galvanostat/potentiostat (Autolab, Netherland) using the conventional three-electrode cell where platinum was used as the auxiliary electrode, Ag/AgCl as reference electrode and ITO as WE, in phosphate buffer saline (PBS, 100 mM, pH 7.2) containing 5 mM $[Fe(CN)_6]^{3-/4-}$.

4. RESULTS AND DISCUSSION

4.1 FT-IR Analysis
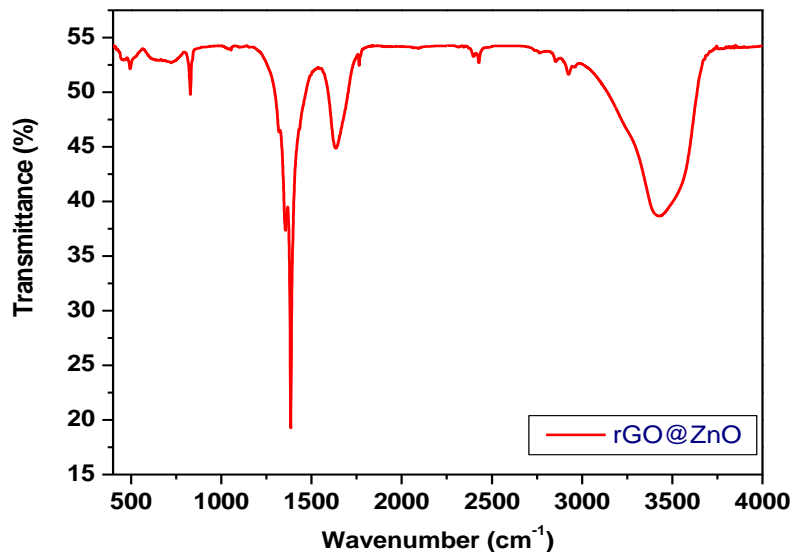
Fig.4.1. FT-IR spectra of rGO@ZnO nanocomposite

The biosynthesized rGO@ZnO nanocomposite was investigated by FT-IR spectroscopy (Fig. 4.1). The spectrum shows a broad peak at 3428 cm^{-1} arising because of O-H group stretching vibrations, and1385 cm^{-1} peak shows C-O groups. At 2859 cm^{-1} and 2923 cm^{-1} peak are due to symmetric and asymmetric vibrations of C-H groups respectively. A peak observed at 1634 cm^{-1} is due to C=O stretching of the carboxylic/carbonyl moiety functional group. The peak at 1046 cm^{-1} shows C-OH stretching and 833 cm^{-1} shows C-O stretching. Also, a solid retention band in under 500 cm^{-1} range is because of the vibrations of Zn-O bonds [30].

4.2 UV-Vis Spectroscopy
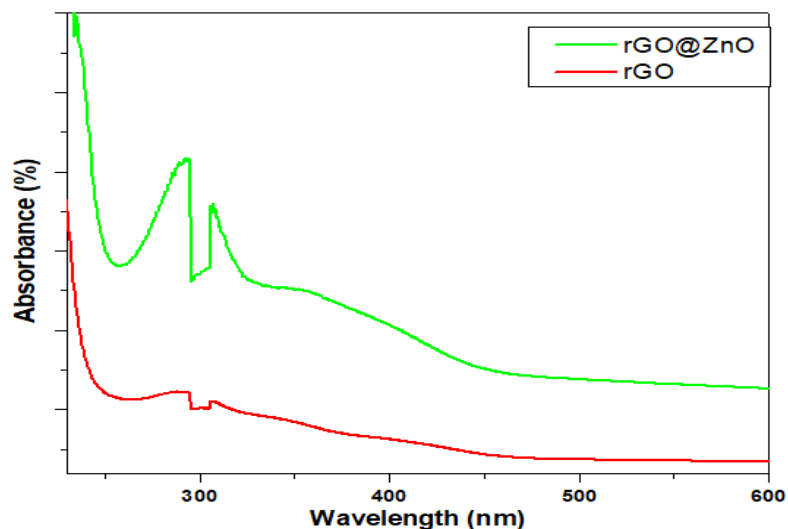
Fig. 4.2.UV-Vis spectrum for rGO@ZnO and rGO

Fig. 4.2 shows the UV- Vis spectra of rGO@ZnO and rGO. The rGO spectra show a redshift from 293 nm to 305 nm because of the removal of oxygen- functional groups from GO and re-establishment of the conjugated structure of rGO. Spectra of rGO@ZnO show a gentle slopping absorption peak at 353 nm due to the presence of ZnO nanoparticles.

4.3 Zeta Potential

The zeta potential results of GO, rGO, rGO@ZnO were observed as -33.1 mV, -26.3 mV, -10 mV, respectively. The high zeta potential of GO was due to the presence of negatively charged –OH and –COOH groups. The value of rGO decreases due to reduction in oxygen functional groups and better dispersion.

4.4 Thermogravimetric Analysis
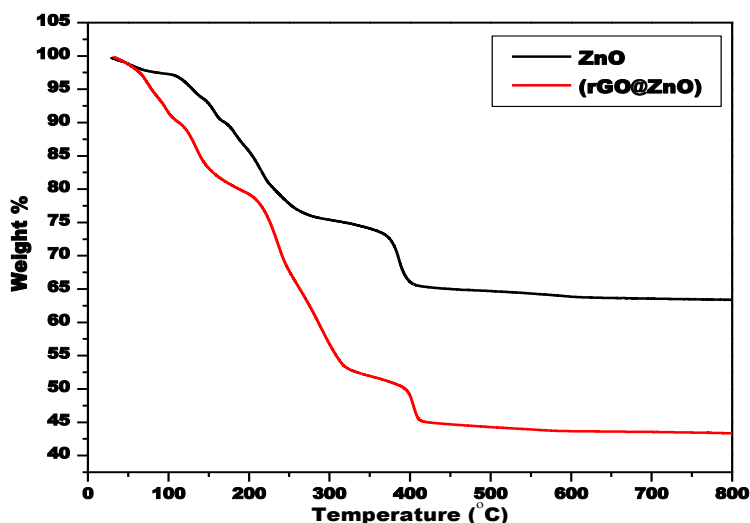
Fig. 4.3. TGA plot for (a) ZnO nanoparticles (b) rGO@ZnO nanoparticles.

TGA curves (Fig 4.3) of ZnO and rGO@ZnO show beginning weight reduction at $100°C$ because of the removal of the water molecules. The significant weight reduction observed at $210^{o}C$-$400^{o}C$ because of the expulsion of oxygen-rich functional groups, for example, CO_2 and CO. Further weight loss, till $420^{o}C$ is due to the removal of remaining oxygen moieties.

4.5 Electrochemical Characterization

Electrochemical studies of the rGO@ZnO/ITO electrode, a-BSA/rGO@ZnO/ITO and BSA/a-BSA/rGO@ZnO/ITO bioelectrode have been performed in phosphate buffer saline (100 mM; pH 7.2; 0.9% NaCl) containing 5 mM of $[Fe(CN_6)]^{3-/4-}$ using cyclic voltammetry (CV) technique [31]. Since BSA is negatively charged and rGO@ZnO nanocomposite forms a positive charge; thus, the main interaction between these two is electrostatic interaction, which leads to the changes in the electrochemical response of the rGO@ZnO [32].
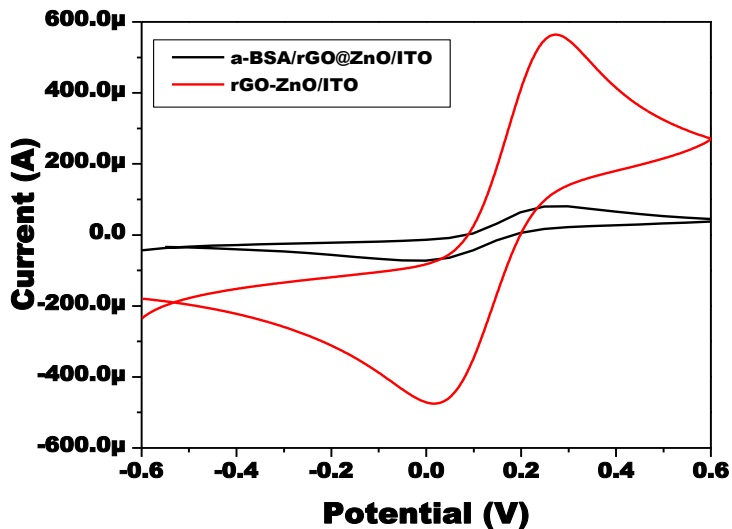
Fig. 4.4. Cyclic voltammograms of anti-BSA/rGO@ZnO/ITO and rGO@ZnO/ITO

Figure 4.4 shows the cyclic voltammetric behavior of rGO@ZnO/ITO and a-BSA immobilized rGO@ZnO/ITO at 50 mV/s. Potential peaks observed at 0.27 V (oxidation) and 0.016 V (reduction) and for a-BSA/rGO@ZnO/ITO oxidation and reduction potential obtained at 0.26 V and -0.034 V, respectively. The peaks are allocated due to the oxidation of Fe^{3+} to Fe^{4+} and the reduction of Fe^{4+} to Fe^{3+} on the electrode. The shift in peak potential values and decrease in peak current values are attributed to the immobilization of a less conductive layer of anti-BSA onto the rGO@ZnO matrix [5].

4.6 Effect of Scan Rate

The variation in the effect of scan rate on CV of (a) rGO/ITO (b) rGO@ZnO/ITO (c) anti-BSA/rGO@ZnO/ITO (d) BSA/rGO@ZnO/ITO has been given in the Fig. 4.5.

Fig.4.5 CVs of (a) rGO/ITO (b) rGO@ZnO/ITO (c) anti-BSA/rGO@ZnO/ITO
(d) BSA/rGO@ZnO/ITO
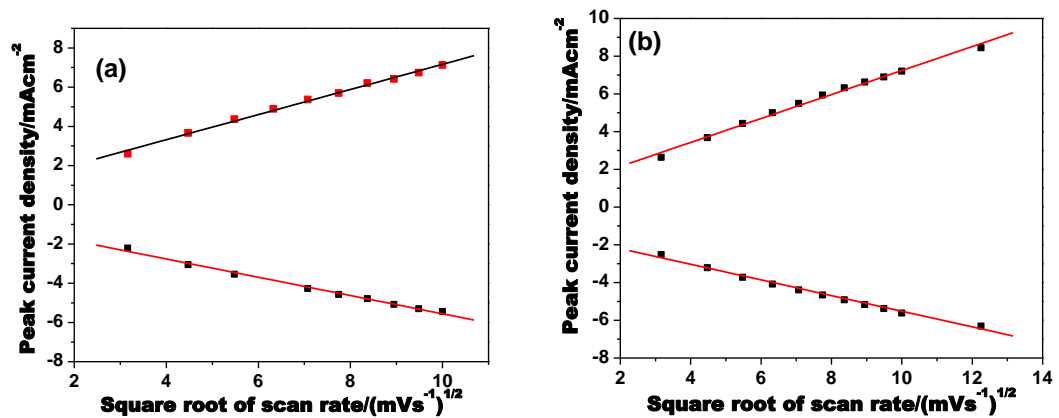
Fig. 4.6 Images showing plots of peak currents vs square root of scan rates for
(a) anti-BSA/rGO@ZnO/ITO (b) BSA/rGO@ZnO/ITO

As the scan rate increased from 10 mV/s- 150 mV/s a linear increase in oxidation peak current and a positive shift in oxidation peak potential is observed in all 4 electrodes. Both peak currents, i.e., I_{pa} & I_{pc} ($I_{pa\ :}$ anodic & I_{pc} : cathodic) increases linearly with increasing scan rate as shown in fig. 4.6, this behavior of peak current variation with scan rate shows surface adsorption controlled kinetics.
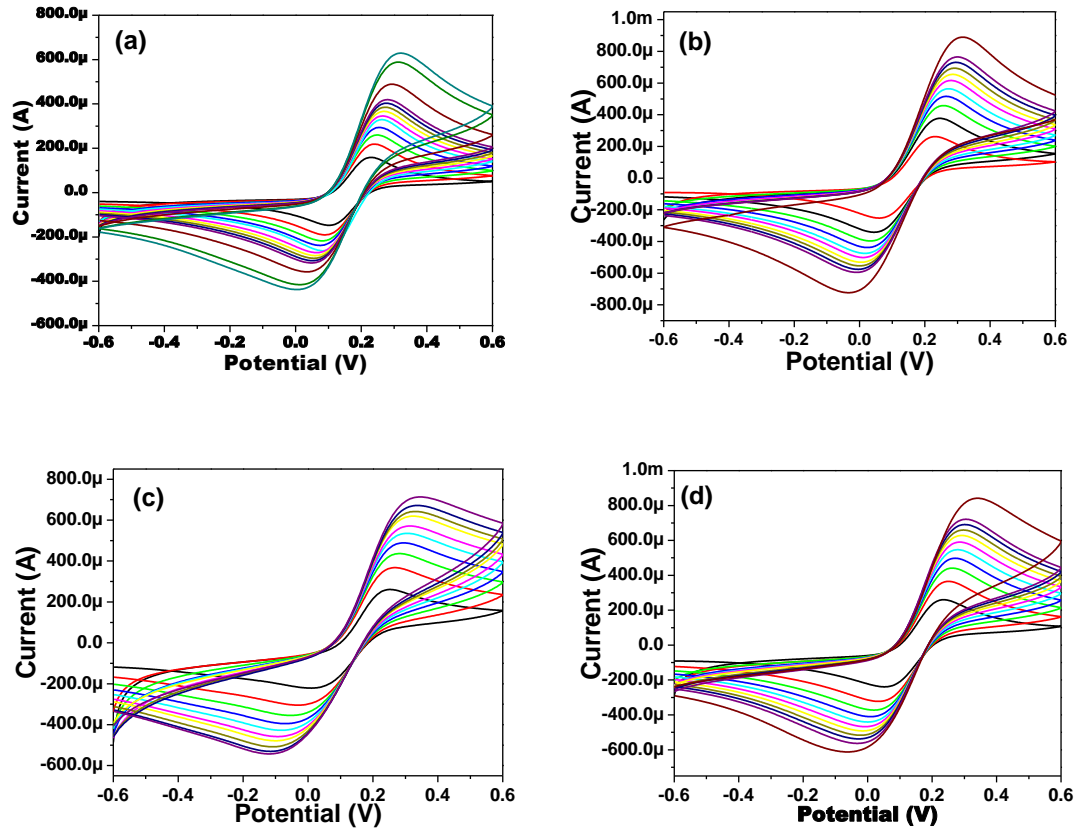
For a-BSA/rGO@ZnO/ITO,

$$I_{pa} = 7.5 \times 10^{-5} + 6.4 \times 10^{-5} \sqrt{\vartheta}$$

$$R = 0.99789$$

$$I_{pc} = -9.0 \times 10^{-5} + -4.6 \times 10^{-5} \sqrt{\vartheta}$$

$$R = 0.99667$$

For BSA/rGO@ZnO/ITO,

$$I_{pa} = 8.86 \times 10^{-5} + 6.35 \times 10^{-5} \sqrt{\vartheta}$$

$$R = 0.9967$$

$$I_{pc} = -1.37 \times 10^{-4} - 4.15 \times 10^{-5} \sqrt{\vartheta}$$

$$R = -0.98919$$

Similarly, from fig. 4.7, a linear correlation was observed for anodic and cathodic peak potentials (E_{pa} & E_{pc}) with respect to the increasing natural logarithm scan rate, linear regression equations depicting the same have been given by below equations.

For rGO@ZnO/ITO,

$$E_{pa} = 0.17413 \ln(\vartheta) + 0.05307$$

$$R = 0.97681$$

$$E_{pc} = 0.17239 \ln(\vartheta) - 0.0627$$

$$R = -0.93934$$

For rGO/ITO,

$$E_{pa} = 0.15615 \ln(\vartheta) + 0.07186$$

$$R = 0.99103$$

$$E_{pc} = 0.14547 \ln(\vartheta) - 0.07639$$

$$R = -0.97488$$
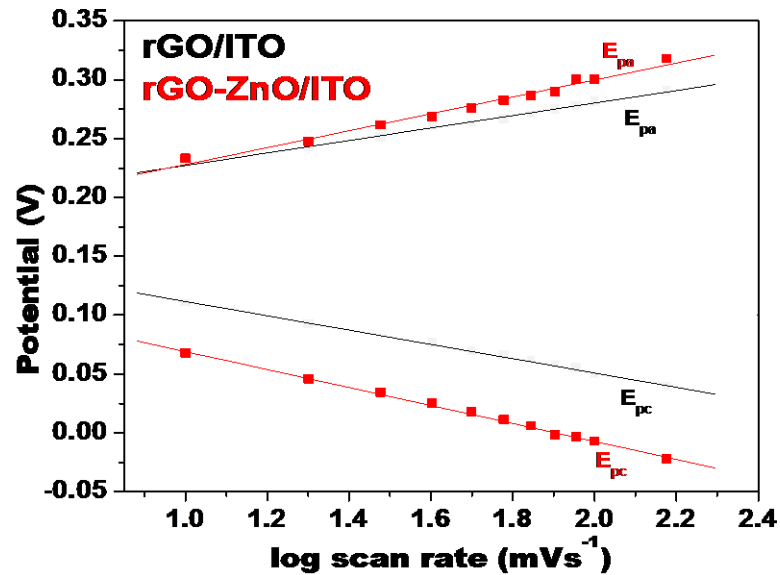
Fig. 4.7 Plots of potential *vs* log of scan rates for rGO/ITO and rGO@ZnO/ITO

At 50 eV, electron transfer rate constant (K_s) of rGO/ITO and rGO@ZnO/ITO electrodes were calculated using Laviron's theory :

Log (K_s) = α log (1-α) + (1-α) log α – log (RT/nFυ) – α (1-α) nFΔE_p/2.3

Where α is the charge transfer coefficient, R is the gas constant, T is the room temperature, ΔE_p is the difference in the peak potential, n is the number of electrons transfer (n=1).

The value of diffusion coefficient (D) and electroactive surface (A) was measured by using the Randles-Sevcik equation

$$I_{pa} = (2.99 \times 10^5)\, \alpha^{1/2}\, n^{3/2}\, A\, C\, D^{1/2}\, \upsilon^{1/2}$$

$$A = S/(2.99 \times 10^5)\, \alpha^{1/2}\, n^{3/2}\, C\, D^{1/2}$$

Table 1. Kinetic Parameters of rGO/ITO and rGO@ZnO/ITO

S. No.	Name of the electrode	Electron transfer coefficient, α	Charge transfer rate constant, K_s/s^{-1}	Effective surface area, A_{eff}/mm^2	Average surface coverage, $\tau/mol\ cm^{-1}$	Diffusion coefficient, D/cm^2s^{-1}
1.	rGO/ITO	0.90	0.1267	0.252	2.763×10^{-8}	1.67×10^{-11}
2.	rGO@ZnO/ITO	0.92	0.0253	0.255	4.791×10^{-8}	5×10^{-11}

4.7 Biosensing Application of anti-BSA/rGO@ZnO/ITO electrode

The electrochemical response of anti-BSA/rGO@ZnO/ITO electrode was studied as a function of increasing concentration of BSA (0.001-30 ng mL^{-1}) in PBS (pH=7.2, 0.9% NaCl) containing 5 mM [Fe(CN)$_6$]$^{-3/-4}$ solution using DPV.
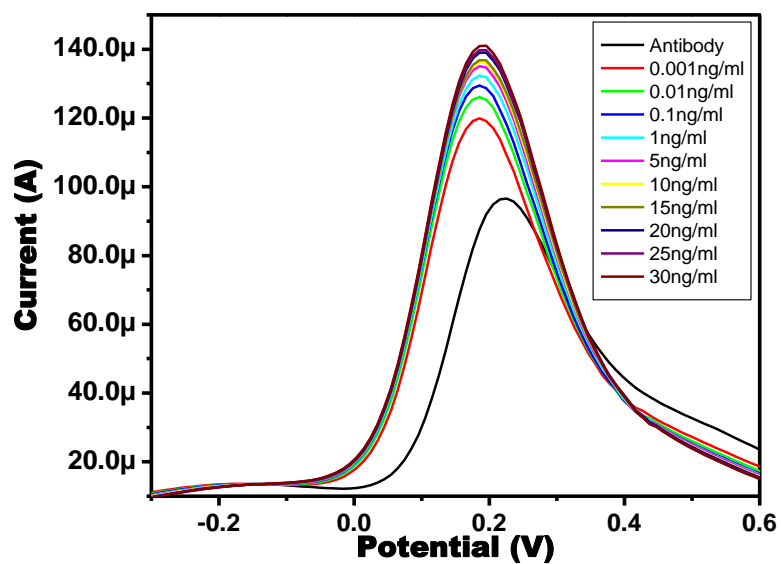

Fig 4.8 Electrochemical response of anti-BSA/rGO@ZnO/ITO as a function of BSA concentration (from bottom to top, 0-30 ngmL^{-1}) using DPV

Fig. 4.8 showing differential pulse voltammetric (DPV) curve depicts the BSA concentrations in the linear range from 0.001 ng mL^{-1} to 30 ng mL^{-1}. From the curve, an increasing trend is obtained with increasing BSA concentration as BSA forms an iron-binding complex in redox couple solution, which results in the formation of iron chelates, which regulates the migration of antigen to the electrode's surface which in turn stimulates the redox reactions.
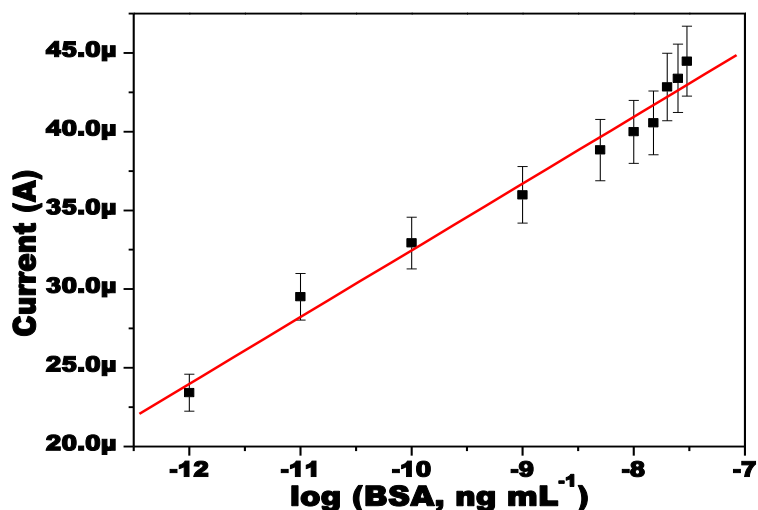
Fig. 4.9.Calibration plot between the magnitudes of current recorded and BSA concentration (0-30 ng mL^{-1}). Error bars represent the standard deviations of repeated determinations.

The calibration plot between current and BSA concentration (0.001-30 ng mL^{-1}) has been shown in fig. 4.9 and follows the Randles-Sevick equation. The sensitivity of the immunosensor was calculated by using the slope equation i.e., y = mx+c where m = $\Delta y/\Delta x$ (slope). The bioelectrode possess a low detection limit of 1 pg mL^{-1} of BSA and a sensitivity of 4.277 µA ng mL^{-1}.

Table 2 shows the comparison of the rGO@ZnO/ITO electrode with other reported sensors for BSA detection. Various sensors have been developed in order to detect BSA with different matrix and techniques of sensing. In our studies, rGO@ZnO biosensor shows the lowest LOD 1 pg mL$^{-1,}$ which can be useful in more efficient detection of BSA than any other methods reported in the literature.

Table2: Comparison of rGO@ZnO/ITO electrode performance with other biosensors reported for BSA detection.

S.No	Matrix	Method	LOD	Ref.
1.	Chitosan with multi-walled carbon nanotubes	DPV	0.028 ng mL^{-1}	[33]
2.	Graphene oxide (GO)	AIE	0.4μM	[34]
3.	Aminopolycarboxyl-modified Ag$_2$S nanoparticles	RLS	112.6 ng mL^{-1}	[35]
4.	Triangular silver nanoplates	LSPR	0.5 ng mL^{-1}	[2]
5.	Amine-functionalized ZnOmicrowires	Micro-electronic chip	15 nM mL^{-1}	[36]
6.	InGap quantum dots	Fluorescence	10^5ng mL^{-1}	[37]
7.	MoS$_2$ nanosheets	CV	6 pg mL^{-1}	[38]
8.	Biosynthesized rGO@ZnO	CV	1 pg mL^{-1}	**Present work**

4.8 Regeneration of immunosensor

The regeneration was proceeded by submersion of the BSA/anti-BSA/rGO@ZnO/ITO electrode for 10 sec in the glycine-HCl buffer (0.1M, pH=3) and washed with PBS solution for interfering with the antigen-antibody acting agent immune complex. A decline in the peak current is seen after every regeneration cycle (Fig.4.10). This is due to the shelling and denaturation of BSA or the structure of rGO@ZnO during the recovery process with glycine–HCl buffer and washing with the expansion of recovery times. This shows that the immunosensor can be reused and recovered for at least 3 times with a relative standard deviation of 4.08% expressing a decent accuracy and high reproducibility. Also, there is 3% decrease in the peak current after the 3rd regeneration cycle.
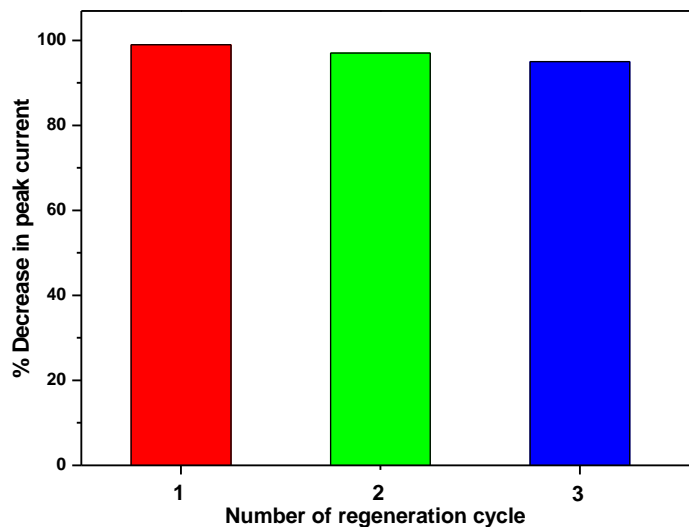
Fig. 4.10 Regenerability of the sensor for repeated detection of BSA over three cycles of uses.

5. CONCLUSION

A highly sensitive electrochemical immunosensor has been fabricated for BSA detection using rGO@ZnO nanocomposite. The rGO@ZnO nanocomposite has been successfully bio-synthesized via an eco-friendly and cost-effective method. The reduction of the material was done using *aloe vera* leaves, which are easily available in tropical areas. The biosynthesized rGO@ZnO was further utilized for the fabrication of biosensor for BSA detection. A linear range of BSA concentration is obtained from 0.001- 30 ng mL^{-1} with a low detection limit (1 pg mL^{-1}) and high sensitivity of 4.277 μA ng mL^{-1}. The bioelectrode can be regenerated and can be reused for atleast 3 times. Further efforts are being made to investigate the performance of the biosensor in clinical samples.

6. FUTURE PROSPECTS

The progressive era has always shown interest in time-saving and user-friendly testing equipment. Therefore, biosensors have proved a useful tool for point of care testing and provided timely and accurate results. Our proposed, fabricated immunosensor is highly promising for the detection of BSA and can be applied to determine cow health and its related products like milk and meat. The response obtained by fabricated immunosensor proved that it could be converted into a portable device for smart detection.

7. REFERENCES

[1]   D. P. Sahu and S. N. Jammalamadaka, "Detection of bovine serum albumin using hybrid TiO2 + graphene oxide based Bio – resistive random access memory device," *Sci. Rep.*, vol. 9, no. 1, pp. 1–10, 2019, doi: 10.1038/s41598-019-52522-w.

[2]   L. L. Zhang, F. F. Ma, Y. F. Kuang, S. Cheng, Y. F. Long, and Q. G. Xiao, "Highly sensitive detection of bovine serum albumin based on the aggregation of triangular silver nanoplates," *Spectrochim. Acta - Part A Mol. Biomol. Spectrosc.*, vol. 154, pp. 98–102, 2016, doi: 10.1016/j.saa.2015.10.019.

[3]   S. Liu, Z. Yang, Z. Liu, and L. Kong, "Resonance Rayleigh-scattering method for the determination of proteins with gold nanoparticle probe," *Anal. Biochem.*, vol. 353, no. 1, pp. 108–116, 2006, doi: 10.1016/j.ab.2006.03.012.

[4]   Z. X. Guo and H. X. Shen, "Highly sensitive assay for protein using resonance light-scattering technique with dibromohydroxyphenylfluorone-molybdenum(VI) complex," *Spectrochim. Acta - Part A Mol. Biomol. Spectrosc.*, vol. 55, no. 14, pp. 2919–2925, 1999, doi: 10.1016/S1386-1425(99)00168-7.

[5]   L. Bhavani Devi, S. Berchmans, and A. B. Mandal, "Highly sensitive detection of proteins using voltammetric assay in the presence of silver nanostructures," *J. Electroanal. Chem.*, vol. 665, pp. 20–25, 2012, doi: 10.1016/j.jelechem.2011.11.013.

[6]   H. H. Nguyen, J. Park, S. Kang, and M. Kim, "Surface plasmon resonance: A versatile technique for biosensor applications," *Sensors (Switzerland)*, vol. 15, no. 5, pp. 10481–10510, 2015, doi: 10.3390/s150510481.

[7]   J. Lin *et al.*, "Raman spectroscopy of human hemoglobin for diabetes detection," *J. Innov. Opt. Health Sci.*, vol. 7, no. 1, 2014, doi: 10.1142/S179354581350051X.

[8]   T. Sato, T. Morishita, T. Hara, I. Suda, and T. Tetsuka, "Near-infrared reflectance spectroscopic analysis of moisture, fat, protein, and physiological activity in buckwheat flour for breeding selection," *Plant Prod. Sci.*, vol. 4, no. 4, pp. 270–277, 2001, doi: 10.1626/pps.4.270.

[9]   J. R. Wišniewski and F. Z. Gaugaz, "Fast and sensitive total protein and peptide

assays for proteomic analysis," *Anal. Chem.*, vol. 87, no. 8, pp. 4110–4116, 2015, doi: 10.1021/ac504689z.

[10] R. L. Varkovitzky, "Assimilation, accommodation, and overaccommodation: An examination of information processing styles in female victims of adolescent and adult sexual assault," *ProQuest Diss. Theses*, vol. 1, no. 6, p. 218, 2012, doi: 10.1038/nprot.2006.202.Using.

[11] S. V. Dzyadevych, V. N. Arkhypova, A. P. Soldatkin, A. V. El'skaya, C. Martelet, and N. Jaffrezic-Renault, "Amperometric enzyme biosensors: Past, present and future," *Itbm-Rbm*, vol. 29, no. 2–3, pp. 171–180, 2008, doi: 10.1016/j.rbmret.2007.11.007.

[12] A. Chaubey and B. D. Malhotra, "Review Mediated biosensors.," *Biosens. Bioelectron.*, vol. 7, pp. 441–456, 2002.

[13] S. K. Krishnan, E. Singh, P. Singh, M. Meyyappan, and H. S. Nalwa, "A review on graphene-based nanocomposites for electrochemical and fluorescent biosensors," *RSC Adv.*, vol. 9, no. 16, pp. 8778–8781, 2019, doi: 10.1039/c8ra09577a.

[14] I. Khalil, S. Rahmati, N. Muhd Julkapli, and W. A. Yehye, "Graphene metal nanocomposites — Recent progress in electrochemical biosensing applications," *J. Ind. Eng. Chem.*, vol. 59, pp. 425–439, 2018, doi: 10.1016/j.jiec.2017.11.001.

[15] F. Parnianchi, M. Nazari, J. Maleki, and M. Mohebi, "Combination of graphene and graphene oxide with metal and metal oxide nanoparticles in fabrication of electrochemical enzymatic biosensors," *Int. Nano Lett.*, vol. 8, no. 4, pp. 229–239, 2018, doi: 10.1007/s40089-018-0253-3.

[16] B. D. Malhotra and C. M. Pandey, *Book-Biosensors : Fundamentals and Applications*. 2017.

[17] Z. Zhao, W. Lei, X. Zhang, B. Wang, and H. Jiang, "ZnO-based amperometric enzyme biosensors," *Sensors*, vol. 10, no. 2, pp. 1216–1231, 2010, doi: 10.3390/s100201216.

[18] P. Malik, R. Shankar, V. Malik, N. Sharma, and T. K. Mukherjee, "Green Chemistry Based Benign Routes for Nanoparticle Synthesis," *J. Nanoparticles*, vol. 2014, pp. 1–14, 2014, doi: 10.1155/2014/302429.

[19] M. Shah, D. Fawcett, S. Sharma, S. K. Tripathy, and G. E. J. Poinern, *Green*

synthesis of metallic nanoparticles via biological entities, vol. 8, no. 11. 2015.

[20] Y. Zhu *et al.*, "Graphene and graphene oxide: Synthesis, properties, and applications," *Adv. Mater.*, vol. 22, no. 35, pp. 3906–3924, 2010, doi: 10.1002/adma.201001068.

[21] S. Moghaddasi, S. K. Verma, and B. Publications, "Aloe vera their chemicals composition and applications: A review a b International Journal of BIOLOGICAL AND MEDICAL RESEARCH," *Int. J. Biol. Med. Res. Int J Biol Med Res. Int J Biol Med Res*, vol. 2, no. 1, pp. 466–471, 2011.

[22] M. Farré, L. Kantiani, and D. Barceló, *Microfluidic Devices: Biosensors*. 2012.

[23] D. Thevenot *et al.*, "Electrochemical biosensors : Recommended definitions and classification (Technical Report) To cite this version : ELECTROCHEMICAL BIOSENSORS : RECOMMENDED," 2014.

[24] T. Gan, Z. Shi, J. Sun, and Y. Liu, "Simple and novel electrochemical sensor for the determination of tetracycline based on iron/zinc cations-exchanged montmorillonite catalyst," *Talanta*, vol. 121, no. January, pp. 187–193, 2014, doi: 10.1016/j.talanta.2014.01.002.

[25] F. R. Simões and M. G. Xavier, *Electrochemical Sensors*. Elsevier Inc., 2017.

[26] A. Jahanban-Esfahlan, A. Ostadrahimi, R. Jahanban-Esfahlan, L. Roufegarinejad, M. Tabibiazar, and R. Amarowicz, "Recent developments in the detection of bovine serum albumin," *Int. J. Biol. Macromol.*, vol. 138, pp. 602–617, 2019, doi: 10.1016/j.ijbiomac.2019.07.096.

[27] M. Kumari, U. K. Singh, P. Singh, and R. Patel, "Effect of N-Butyl-N-Methyl-Morpholinium Bromide Ionic Liquid on the Conformation Stability of Human Serum Albumin," *ChemistrySelect*, vol. 2, no. 3, pp. 1241–1249, 2017, doi: 10.1002/slct.201601477.

[28] A. M. Dimiev and J. M. Tour, "Mechanism of graphene oxide formation," *ACS Nano*, vol. 8, no. 3, pp. 3060–3068, 2014, doi: 10.1021/nn500606a.

[29] G. Lee and B. S. Kim, "Biological reduction of graphene oxide using plant leaf extracts," *Biotechnol. Prog.*, vol. 30, no. 2, pp. 463–469, 2014, doi: 10.1002/btpr.1862.

[30] S. A. Hosseini and S. Babaei, "Graphene oxide/zinc oxide (GO/ZnO) nanocomposite as a superior photocatalyst for degradation of methylene blue

(MB)-process modeling by response surface methodology (RSM)," *J. Braz. Chem. Soc.*, vol. 28, no. 2, pp. 299–307, 2017, doi: 10.5935/0103-5053.20160176.

[31] G. Ertürk, D. Berillo, M. Hedström, and B. Mattiasson, "Microcontact-BSA imprinted capacitive biosensor for real-time, sensitive and selective detection of BSA," *Biotechnol. Reports*, vol. 3, pp. 65–72, 2014, doi: 10.1016/j.btre.2014.06.006.

[32] M. Qi *et al.*, "Adsorption and electrochemical detection of bovine serum albumin imprinted calcium alginate hydrogel membrane," *Polymers (Basel).*, vol. 11, no. 4, 2019, doi: 10.3390/polym11040622.

[33] H. J. Chen, Z. H. Zhang, L. J. Luo, and S. Z. Yao, "Surface-imprinted chitosan-coated magnetic nanoparticles modified multi-walled carbon nanotubes biosensor for detection of bovine serum albumin," *Sensors Actuators, B Chem.*, vol. 163, no. 1, pp. 76–83, 2012, doi: 10.1016/j.snb.2012.01.010.

[34] X. Xu, J. Huang, J. Li, J. Yan, J. Qin, and Z. Li, "A graphene oxide-based AIE biosensor with high selectivity toward bovine serum albumin," *Chem. Commun.*, vol. 47, no. 45, pp. 12385–12387, 2011, doi: 10.1039/c1cc15735c.

[35] H. Pan, X. Tao, C. Mao, J. J. Zhu, and F. Liang, "Aminopolycarboxyl-modified Ag2S nanoparticles: Synthesis, characterization and resonance light scattering sensing for bovine serum albumin," *Talanta*, vol. 71, no. 1, pp. 276–281, 2007, doi: 10.1016/j.talanta.2006.03.057.

[36] A. Sanginario, V. Cauda, A. Bonanno, K. Bejtka, S. Sapienza, and D. Demarchi, "An electronic platform for real-time detection of bovine serum albumin by means of amine-functionalized zinc oxide microwires," *RSC Adv.*, vol. 6, no. 2, pp. 891–897, 2016, doi: 10.1039/c5ra15787k.

[37] P. Kumar, A. Deep, S. C. Sharma, and L. M. Bharadwaj, "Bioconjugation of InGaP quantum dots for molecular sensing," *Anal. Biochem.*, vol. 421, no. 1, pp. 285–290, 2012, doi: 10.1016/j.ab.2011.10.037.

[38] M. Kukkar, A. Sharma, P. Kumar, K. H. Kim, and A. Deep, "Application of MoS2 modified screen-printed electrodes for highly sensitive detection of bovine serum albumin," *Anal. Chim. Acta*, vol. 939, pp. 101–107, 2016, doi: 10.1016/j.aca.2016.08.010.